THE DYNAMICS OF HEAD AND NECK IMPACT

AND ITS ROLE IN INJURY PREVENTION AND THE COMPLEX CLINICAL PRESENTATION OF CERVICAL SPINE INJURY

Barry S. Myers, M.D., Ph.D. and Roger Nightingale, Ph.D.

Injury and Orthopaedic Biomechanics Laboratory
Department of Biomedical Engineering,
Department of Biological Anthropology and Anatomy
Division of Orthopaedic Surgery
Duke University

ABSTRACT

This paper reviews our research on catastrophic head impact compression neck injury. On the basis of these experiments, a biomechanical model of the spine is developed in which the complex clinical presentation of cervical spine injuries may be better understood. This includes the significance of head rebound, head and neck decoupling, cervical spine buckling, cervical injury mechanisms, basilar skull fractures, cervical injury classification, and cervical spine tolerance. Specifically, we hypothesize that impact injury should be modeled as the dynamic response of two large masses coupled by a segmented curved beam-column comprised of seven small masses with interposed nonlinear viscoelastic flexibility elements. These impact data also provide insights into the effects of the padding on the mitigation of head and neck injury.

CATASTROPHIC CERVICAL SPINAL INJURY has remained among the most difficult and socially significant impact injury problems in structural biomechanics. While these injuries occur through a variety of mechanisms, including direct and indirect loading, and contact and non-contact loading, head contact resulting in compression-bending neck loading remains among the most common mechanisms of injury. The volume of literature which has been devoted to the characterization of cervical spinal impact injury is large, and has been recently been reviewed in detail (Myers and Winkelstein, 1995). Despite this collection of writing, considerable confusion remains as to the basic mechanisms which result in catastrophic cervical spinal injuries including: the effects of end condition; the relationships between head motion and injury mechanisms; the effects of head, neck, and torso inertia; the role of buckling in injury, and the effects of the initial orientations of the head, neck, and torso relative to the impact surface. Although previous studies have examined these variables and provided invaluable insights into the dynamic behavior of the cervical spine, few have had the long term support necessary to obtain the meaningful sample size for statistically confident conclusions.

The failure of the classical static approach to neck injury is best illustrated by efforts to classify catastrophic injuries. Classically, it is suggested that in order to produce a lower cervical flexion injury, the head must be flexed, causing the entire spine to flex until a motion segment is loaded beyond its tolerance (Harris et al., 1986). However, analysis of real-world head-impact neck injuries frequently results in paradoxic observations in which head motion is not consistent with the classical thinking on injury mechanism. Consider the following case history (Figure 1). A restrained front seat passenger in a driver side leading rollover suffers a blow to the head during the inverted impact of the roof to the ground. The impact resulted in a lower cervical bilateral facet dislocation, a posterior arch fracture of the atlas and a posterior arch fracture of the axis (a Hangman's fracture). In this case, a midsagittal laceration anterior to the head vertex, but posterior to the hairline, clearly defined the point of head impact. This illustrates an example of multiple noncontiguous spinal injuries in which the injury mechanisms differ (i.e. a lower cervical compression-flexion injury in association with contiguous upper cervical compression-extension injuries). This cannot be explained on the basis of a simple head motion and is not consistent with the site of head impact, which one would expect to cause the head to move in extension.

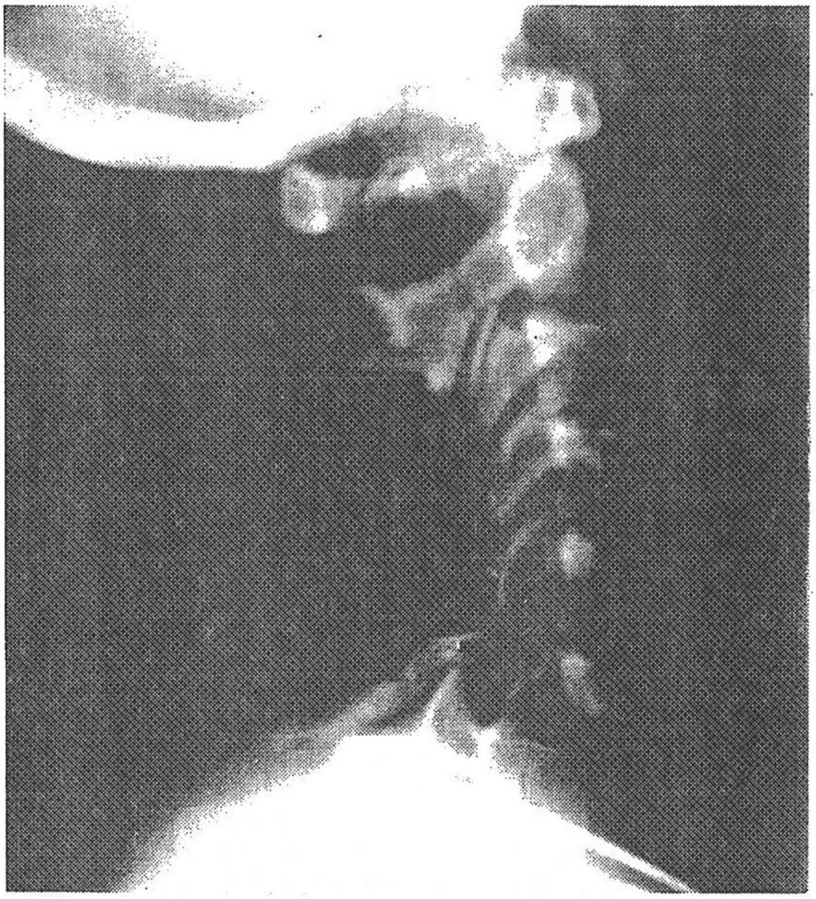

FIGURE 1 Lateral X-ray illustrating a C6-C7 bilateral facet dislocation resulting from compression-flexion loading, and posterior element fractures of the atlas and axis from compression-extension loading. Both injuries were the result of a single impact anterior to the head vertex, and illustrate the poor relationship between the motions of the head in impact and the motions and injuries of the spine.

Of equal importance to characterizing injury is the prevention of injury. It is widely assumed that energy absorbing devices which are designed to reduce the severity and incidence of head injury also reduce the risk for neck injury. Such devices include helmets, airbags, American football tackling blocks, and padded surfaces on vehicle interiors. Despite this belief, reduction of neck injury through the use of padding has never been demonstrated in any experimental or epidemiological study. On the contrary, a number of studies have shown that padded surfaces have no effect on cervical spine injury risk (Alem et al., 1984; Nusholtz et al., 1983, Pintar et al., 1990), and others have presented evidence that they can increase the risk (Hodgson and Thomas, 1980; Mertz et al., 1978; Myers et al., 1991; Torg et al., 1976; Yoganandan et al., 1986). Nusholtz et al. (1983) performed a study using whole cadavers and concluded that energy absorbing materials "did not necessarily reduce the amount of energy transferred to the head, neck, and torso or the cervical damage produced". Hodgson and Thomas (1980) conducted impact tests on whole cadavers and found that distributed impacts (arising from padded impact surfaces) tend to "grip" the head and strongly influence the mechanism of injury. A quasi-static experiment by Myers et al. (1991) showed a dramatic increase in cervical spine stiffness and injury risk with increasing constraints on the motion of the head. Based on these results, they concluded that restrictions on head motion may increase the risk for cervical spine injury by not allowing the head and neck to move out of the path of the following torso. Despite these supportive arguments, there have been no studies which have studied the effects of padding by systematically varying the material characteristics of the impact surface. Therefore, one of the goals of our research is to create a realistic head impact environment in which we can test the hypothesis that padded impact surfaces can increase the risk and severity of cervical spine injury by constraining the motion of the head.

Clearly, if we are to become more effective in preventing cervical spine injuries, a cogent understanding of how they occur must first be achieved. Based on our experience, we hypothesize that the cervical impact behavior may be characterized as the impulsive response of a curved segmented beam column comprised of seven small masses, coupled by nonlinear viscoelastic elements, bounded between two large masses with significant rotary inertia. Fortunately, over the last fifteen years, a renewed interest in determining the basic biomechanics of neck injury has developed in the United States from both the Centers for Disease Control, and the National Highway Traffic Safety Administration allowing us the opportunity to test our hypothesis. It is therefore, the purpose of this paper to review our research on catastrophic head impact neck injury which support this premise (Myers et al., 1997; Nightingale et al., 1996a, 1996b, 1997a, 1997b), to provide a biomechanical framework upon which the mechanisms of cervical spine impact injuries occur, and to discuss a framework upon which injury prevention strategies can be developed and refined.

MATERIALS AND METHODS

Experimental Apparatus

An experimental apparatus was designed to model cervical spine injury resulting from vertical head impact with a following torso (Figure 2). A steel carriage was mounted to a drop track using two linear bearing sliders and was weighted to simulate an effective torso mass of 16 kg. The value for the torso mass is based on the GEBOD output for the 50th percentile male upper torso and is an estimate of the portion of the total body mass which acts on the neck during dynamic loading. The specimen preparations were mounted to the carriage in an inverted position.

The impact surface was a 4 cm thick steel anvil with a diameter of 15.25 cm. Variation in impact angle about the y-axis (that axis normal to the sagittal plane) was achieved by mounting the anvil on a locking clevis. The impact angle was varied between -15° (posterior head impact) and +30° (anterior head impact), according to the sign convention shown in Figure 1. The anvil was covered with 3 mm of Teflon sheet to simulate impacts onto a rigid, frictionless surface. Impacts onto a padded surface were

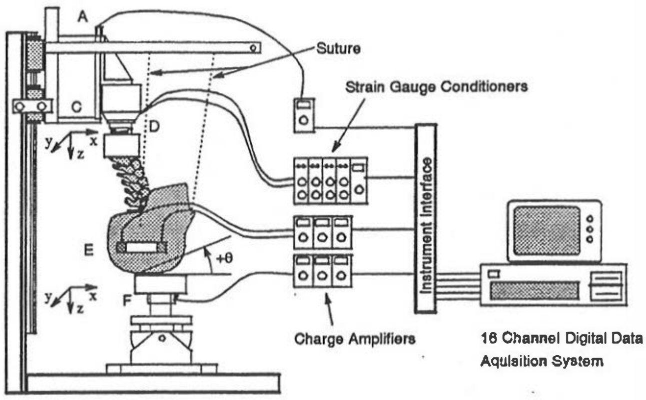

FIGURE 2 A diagram of the test apparatus showing the accelerometer on the torso mass (A), the optical velocity sensor (B), the carriage and torso mass (C), the six-axis load cell at T1 (D), the head accelerometers (E), and the anvil and three-axis load cell (F).

simulated by attaching foams to the anvil with duct tape. The Teflon covered steel surface simulated the unconstrained head end condition in 10 tests. A more constrained head end condition was simulated in the remaining tests (n=12) using either an expanded polystyrene foam (EPS) (E =2096.1 kPa, σ_y =206.2 kPa, ρ =0.0284 g/cm^3) or a less stiff, open cell polyurethane foam (OPU) (E =158.6 kPa, σ_y=7.0 kPa, ρ =0.0277 g/cm^3).

Multiaxis transduction was used to fully quantify the forces and moments acting on the head and neck during the impact event. Head impact forces were quantified using a Kistler 9067 three-axis piezoelectric load cell mounted under the impact surface. A GSE Model 6607-00 six-axis load cell mounted to the specimen was used to measure forces and moments at T1. A PCB 302A02 uniaxial accelerometer measured torso deceleration. Sagittal plane kinematics were quantified using two PCB 306A06 accelerometers which were mounted to the head of the specimen. Impact velocity was recorded using an MTS optical sensor. The sixteen channels of transducer data were sampled at 62.5 kHz using a PC-based acquisition system. Each test was also imaged using a Kodak Ektapro EM-2 digital camera at 1000 frames per second.

Specimen Preparation

Unembalmed human heads with intact spines were obtained shortly after death. All specimen handling was performed in compliance with CDC guidelines (Cavanaugh et al., 1990). The specimens were sprayed with calcium buffered isotonic saline, sealed in plastic bags, frozen and stored at -20°. All donor medical records were examined to ensure that there were no preexisting conditions, such as degenerative diseases or spinal pathologies, which could affect the structural responses of the specimens. Donor age ranged from 35 to 80 years.

The specimens were prepared for testing in a 100 percent relative humidity chamber. The muscular tissues were removed while keeping all the ligamentous structures intact (with the exception of the ligamentum nuchae). The specimens were transected at T3-T4 and the bottom two vertebrae were cleaned, defatted, and cast into aluminum cups with reinforced polyester resin. Care was taken that the most rostral uncast vertebra was free of resin and was allowed full range of motion. The C7-T1 intervertebral disc was oriented at 25 degrees to horizontal to preserve the resting lordosis of the cervical spine (Matsushita et al., 1994). Following casting, a triaxial accelerometer array was attached to exposed parietal bone using dental acrylic and bone screws. A jig was used to ensure that the array was positioned parallel to the sagittal plane. The position of the array relative to the Frankfort anatomical plane was determined radiographically using the auditory meati and the inferior margins of the orbits. Finally, photographic target pins (4.0 mm diameter) were inserted in the anterior vertebral bodies, the spinous processes, and lateral masses of C2-C7. The pins were used for photogrammetric analysis of the vertebral motions.

Experimental Protocol

Cadaveric specimens were inverted and mounted to the carriage of the drop track system in the anatomically neutral position. Break-away sutures were passed through the ear lobules and nasal septum and were tied to the suspension frame to maintain the neutral orientation of the cervical spine. Each specimen was raised to the desired height and the cervical spine was mechanically stabilized by manual exercise through a flexion-extension range of 60° for fifty cycles (McElhaney et al., 1983). The specimens were dropped from a height of 0.53 m, which was less than that required to cause a skull fracture, yet sufficient to produce cervical spine injury (McElhaney et al., 1979). Following impact testing, anteroposterior and lateral radiographs were obtained and the specimen was disarticulated at O-C1 and the head was weighed. To document the injuries, dissection was performed on both the heads and cervical spines.

Data Analysis

All transducer data were uploaded to a Sun SparcStation 2 for analysis. Digital filtration was performed in accordance with the Society of Automotive Engineers standard for head and neck impacts (SAE J211b Class 1000). In order to determine inertial head loading and evaluate the risk of head injury, linear acceleration of the center of gravity of the head was determined from the head mounted accelerometer array.

In impact testing, events other than material failure can be associated with a drop in the axial force with time. These include buckling, slip of the head on the impact surface, and unloading of the neck due to rebound of the torso. The following criteria were used to define mechanical failure and relate mechanical failure to the occurrence of injury. Each decrease in force with increasing time was evaluated. The high speed images were coregistered to the load cell data and were analyzed to define the kinematics of each motion segment at the time of decreasing load. A decrease in load was related to a specific injury if the kinematics and injury mechanism were mutually consistent at the time of the decrease in load. Decreases in load as a result of slip at the head-impact surface were excluded by examination of image and head acceleration data. Decreases in load associated with increases in length of the neck were considered to be mechanical unloading and were similarly excluded. Any decrease in load with a concomitant increase in bending moment which also demonstrated a rapid transition from one mode of deformation to another mode of deformation on high speed images, and no evidence of injury at the site of the transition was defined as a stable buckle.

The clinical stability of a cervical spine injury is a measure of its severity. Stable injuries generally do not result in a progressive neurological deficit and are treated conservatively. Unstable injuries are much more likely to have neurological involvement and are treated by open or closed reduction and fixation. The stability of all the injuries produced in the drop tests was assessed using two methods. First, the injured motion segments were manipulated and obvious gross motions were defined as unstable. Second, the injuries were evaluated using the "one column plus one element" stability criteria outlined by Panjabi et al. (1979). If all the elements of the anterior column (anterior longitudinal ligament, disc, and posterior longitudinal ligament) and any element of the posterior column (facets, ligamentum flavum, interspinous ligament, and supraspinous ligament) are disrupted, then the injury is considered to be potentially unstable. Similarly, the injury is classified as unstable if the posterior column and any element of the anterior column are disrupted.

The impulse of the compressive component of force at T1 was calculated for all the impacts by integrating the axial force history. Differences in axial impulse between the padded and rigid tests were evaluated using two-way ANOVA. The effect of padding on the frequency of injury was examined using a χ^2 comparison of proportions for two independent samples with a continuity correction. The effects of padding on the peak head and neck forces were examined using t-tests.

RESULTS

Using this test system, a total of 22 impact tests have been performed to date, producing basilar skull fractures and cervical spine injuries in 16 cases (Tables 1 and 2). Cervical spine injuries included anterior disc tears, anterior longitudinal ligament ruptures, Jefferson fractures, Hangman's fractures, odontoid fractures, burst fractures, facet dislocations, and posterior element fractures.

TABLE 1: Subject Data and Drop Test Results

TEST	Age, Sex	Vel. (m/s)	Angle (deg.)	Res.[a] Head Force (N)	Axial[b] Neck Force (N)	Res.[c] Neck Force (N)	Time[d] (msec)	Impulse (N · s)	Lag (msec)	HIC
Rigid surface										
N05-R+30	36,M	3.23	Ant. (+30)	8790	1552	1593	8.3	35.9	1.8	497
N18-R+15	–,M	3.26	Ant. (+15)	7498	1863	1895	6.4	62.6	6.4	1935
D41-R+15	69,M	3.11	Ant. (+15)	8604	NI	NI	NI	56.6	2.0	–
I32-R+15	78,M	3.18	Ant. (+15)	8234	2416	2612	3.9	38.9	1.9	1361
N26-R+0	65,M	2.43	Vertex (0)	7638	NI	NI	NI	47.7	1.5	–
N24-R+0	62,M	3.20	Vertex (0)	8566	1839	1973	2.2	40.7	2.2	–
N22-R+0	71,M	3.26	Vertex (0)	8111	1955	2120	6.5	46.9	6.5	490
N11-R-15	55,M	3.14	Post. (-15)	11621	NI	NI	NI	24.1	2.2	543
N13-R-15	35,F	3.28	Post. (-15)	5615	NI	NI	NI	20.6	1.3	704
UK3-R-15	62,M	3.13	Post. (-15)	5093	NI	NI	NI	30.7	1.0	1783
Padded surface										
N21-P+30	61,M	3.13	Ant. (+30)	1760	1632	1662	14.8	42.7	5.3	50
N23A-P+30	46,M	3.03	Ant. (+30)	3608	NI	NI	NI	39.7	5.8	77
N23B-P+30	46,M	3.51	Ant. (+30)	3857	2240	1698	18.7	31.7	7.5	197
I08-P+15	80,M	3.15	Ant. (+15)	5946	2915	2918	30.5	78.6	4.2	110
I11-P+15	63,F	3.20	Ant. (+15)	3115	967	972	14.0	71.9	4.6	118
I04-P+15	63,M	3.19	Ant. (+15)	3383	1675	1698	18.0	74.1	3.8	
N03-P+0	75,M	3.08	Vertex (0)	5664	3172	3509	18.2	62.7	2.7	84
N02-P+0	75,F	3.14	Vertex (0)	3452	715	793	14.7	76.0	2.6	122
D40-P+0	53,F	3.16	Vertex (0)	4187	1438	1440	16.7	81.1	1.7	
N19-P-15	42,F	3.07	Post. (-15)	2604	1011	1037	18.8	22.6	9.0	175
NA2-P-15	61,M	3.16	Post. (-15)	4749	1968	2091	15.6	35.1	4.2	270
I25-P-15	59,M	3.07	Post. (-15)	5963	2558	2574	18.4	39.7	2.9	384

NI The specimen had no injury.
[a] Peak resultant head force.
[b] The magnitude of axial neck force at injury.
[c] The magnitude of the resultant neck force at injury.
[d] The the elapsed time between impact and injury.

The impact dynamics of the head and neck are bimodal and reflect the vibrations of a two mass system with an interposed poorly coupled viscoelastic spring striking an impact surface (Figure 3). For the rigid impacts, Mode 1 is attributed almost entirely

TABLE 2: Injury Results

TEST	Pathology	Class (Allen, 1982)	Stability	Head Motion
Rigid surface				
N05-R+30	C3 burst fx.,	VC	unstable	extension
	C3–C4 disc and ALL,	DE	stable	
	C4–C5 ALL	DE	stable	
N18-R+15	C1 lateral mass fracture,	VC	stable	extension
	C2 hangman's, C2-3 disc and ALL,	DE	unstable	
	C6-7 bilat. facet dislocation	DF	unstable	
D41-R+15	None	–	–	extension
I32-R+15	C5-6 disc, L capsular lig., ALL	DE	stable	extension
N26-R+0	None	–	–	extension
N24-R+0	C1 2 part posterior arch fracture,	CE	stable	flexion
	C2 hangman's fracture	DE	stable	
N22-R+0	C1 3 part comminuted fracture	VC	unstable	extension
N11-R-15	None	–	–	flexion
N13-R-15	None	–	–	flexion
UK3-R-15	None	–	–	flexion
Padded surface				
N21-P+30	C1 anterior ring fx.,	CF	stable	extension
	C4 spinous process fx.,	CE	stable	
	C5 spinous process fx.,	CE	stable	
	C5–C6 disc, left capsular lig. and ALL	DE	stable	
N23A-P+30	None	–	–	extension
N23B-P+30	C1 2 part right aspect fx.,	VC	stable	extension
	C3–C4 disc and ALL,	DE	stable	
	C4–C5 disc and ALL	DE	stable	
I08-P+15	C2 hangman's fracture and burst	DE	unstable	none
I11-P+15	C2 type III dens + comminution,	–	unstable	none
	C4 body, R lamina	VC	stable	
I04-P+15	C1 2 part posterior arch fracture,	CE	stable	none
	C2 hangman's, C2-3 disc, ALL,	DE	unstable	
	C7-T1 posterior ligs.	DF	stable	
N03-P+0	C4-5 capsular lig.,	–	stable	flexion
	C5-6 disc,	DE	stable	
	C6-7 bilat. facet dislocation	DF	unstable	
N02-P+0	C1 ant. ring,	CF	stable	none
	C2 hangman's + type III dens,	DE	unstable	
	C6 R lamina and pedicle,	VC	stable	
	C7 burst	VC	unstable	
D40-P+0	C1 3 part comminuted fracture,	VC	unstable	none
	C3-4 disc, ALL, spinous proc.,	DE	stable	
	C5 (burst), C5-6 PLL,	VC	unstable	
	C6 R lamina and pedicle	VC	stable	
N19-P-15	C2-3 disc, ALL, C2 ant. avul. fracture,	DE	stable	flexion
	C3-4 disc, ALL C3 ant. avul. fracture	DE	stable	
NA2-P-15	C3-4 disc, ALL, L capsular lig.,	DE	stable	flexion
	C5-6 disc, ALL	DE	stable	
I25-P-15	C1-2 L capsular lig.,	–	stable	flexion
	C3-4 disc, ALL, PLL, L capsular lig.	DE	unstable	

* Upper cervical spine injuries were classified using a system similar to that of Allen et al. (1982)

to stopping the head and had a duration of 4.3±1.6 milliseconds. During the first half of this head inertial loading mode, the head impact force reached a maximum with no concomitant neck force (Figure 3). Neck loading at T1 was not observed until the latter half of Mode 1. For the padded impacts, the head contact times during Mode 1 were significantly increased. Therefore, the first mode contained loading by the torso in addition to the force required to stop the head. The inertia and compliance of the head mass caused rebound loading. Head rebound forces on the order of 10 to 35% of the peak head force were commonly observed, indicating that in impact, the neck must manage both the momentum of the torso and the head (Figure 4). Mode 1 durations for the padded impacts could not be calculated because the increased coupling of the head and cervical spine resulted in less separation between modes. For both impact surfaces, Mode 2 represents loading of the impactor surface by the head, cervical spine, and the effective torso mass. The duration of this neck impact surface loading mode for the rigid impact was 27.3±14.3 msec. In all the tests there was a delay in the onset of measured neck load with respect to the head load. This lag in response at T1 was 1.6±0.3 msec for the rigid impacts which was significantly different than the 4.7±1.3 msec for the padded impacts (p<0.001, Table 1). The lag is evidence that the head and cervical spine are not coupled during the first half of the head impact mode.

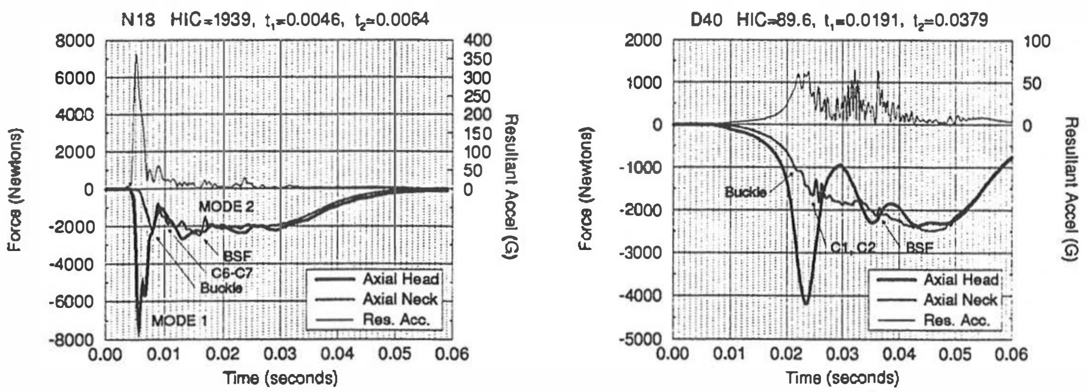

FIGURE 3 Magnitude of the head and neck axial forces, and the head center of gravity acceleration for an impact into a rigid surface oriented at +15° (anterior) (left) and into a padded surface oriented at +0° (right). A bimodal response consisting of a head inertial deceleration mode (Mode 1), and a neck impact surface loading mode (Mode 2) are seen in both the padded impact and the unpadded impact. Analysis of the rigid impact (left) kinematic data revealed a stable buckle followed by a C6-C7 bilateral facet dislocation, and a basilar skull fracture. Addition of padding significantly lowered the head accelerations, HIC, and the Mode 1 head impact forces, however the bimodal response was still observed. Addition of padding also increased the head contact time in the impact surface. Interesting, the basilar skull fracture occurred during the neck impact surface loading mode (Mode 2).

Head motion was not related to injury mechanism. Cervical spine injuries were produced within 9 msec following head contact with a rigid surface and in less than 20 msec in all but one of the padded surface impacts. In contrast, significant head motions, as characterized by rotations greater than 20°, did not occur until between 20 msec and 100 msec following head impact (larger times in the padded impacts and shorter times in the rigid impacts). During the initial phases of impact, the heads were observed to undergo small flexion or extension motions which were not in the direction of the final motion owing to the curvature of the head. The final head motions, the kind which would be observable on a 60 Hz recording or to an observer, were directly related to the point of impact. Specifically, for head impacts forward of 15°, the final head motion was extension rotation. For impact surfaces oriented at 15° and posterior, the final head motion was flexion. Analysis of the injuries and the mechanism of injury as determined by local spinal kinematics, and force analysis was unrelated to the final head

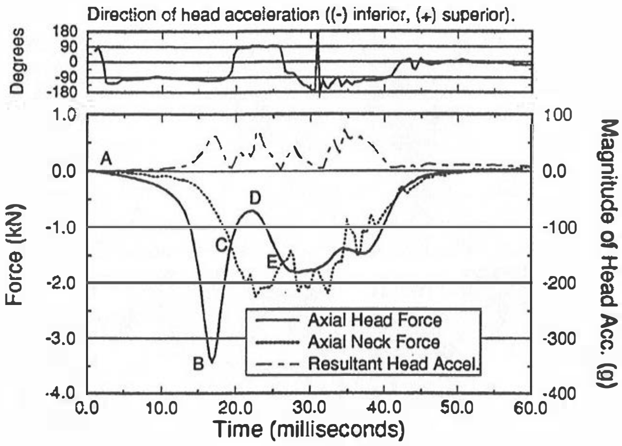

FIGURE 4 Vertical force and acceleration history for the head and neck. Initially, the head hits the contact surface, large head forces accelerate the head up (negative accelerations). After C, the vertical force of the neck driving the head back down into the impact surface exceeds the head-impact surface force, and the head is driven down (positive acceleration) into the impactor by the neck. In that regard, the neck loading reflects inertial contributions of the head and the torso.

motions (Table 2). Injuries produced prior to the head flexion motion included eight extension injuries, one compression injury, and one flexion injury. Injuries produced prior to the head extension motion included, nine extension injuries, four compression injuries and two flexion injuries. Of those impacts not resulting in significant head motions, compression, extension and flexion injuries were produced. Further, head motion was unable to explain the occurrence of multiple noncontiguous injuries in which differing injury mechanisms were observed.

Dynamic buckling of the cervical spine following head impact was observed in each impact within a 3 to 8 msec interval (Figure 3). The buckle was characterized by a rapid transition from a compression mode of deformation to a bending mode of deformation (Figure 5). Because the buckle was observed in specimens without injury, and because the injured spines demonstrated post-bucking stability prior to injury, we concluded that the buckle did not result in material failure. Deforming as a fixed-pinned precurved member, the spine underwent a characteristic postbuckled configuration with midcervical extension and lowermost cervical flexion, while the upper cervical spine flexed, extended, or remained aligned and compressed. Unlike head motion, the post-buckled deformation and resultant force location are able to explain the mechanism and patterns of injury (Figure 6).

Interestingly, three basilar skull ring fractures were detected following craniotomy and removal of the brain (N18, D40, and I11). No cranial vault fractures were detected. In each of the three cases, cervical injuries were also detected. Two cases (N18, and D40) involved contiguous fractures of C1, while the third (I11) had noncontiguous cervical injuries. Each basilar skull ring fracture originated in the dorsum sellae or the occipital clivus anteriorly. The fractures propagated bilaterally through the sphenoid bone, temporal bone, or adjoining sutures. The fractures then propagated posteriorly around, or into, the foramen magnum forming either complete (D40 and N18) or incomplete ring fractures (I11). The rostral-most (anterior) portion of each fracture was displaced into the cranial vault by 3 to 5 mm. The caudal-most (posterior) portion of each fracture showed less displacement. Each fracture was mechanically stable to palpation as a result of soft tissue attachments, incomplete fractures, and interdigitation of the fracture fragments. With effort, the basilar skull fragment could be displaced into the vault. Because of the mechanical stability of the fracture and minimal displacement of the posterior portions of the fractures, the injuries were not readily apparent on external examination of the skull following craniocervical dislocation, nor were they detected on plain films.

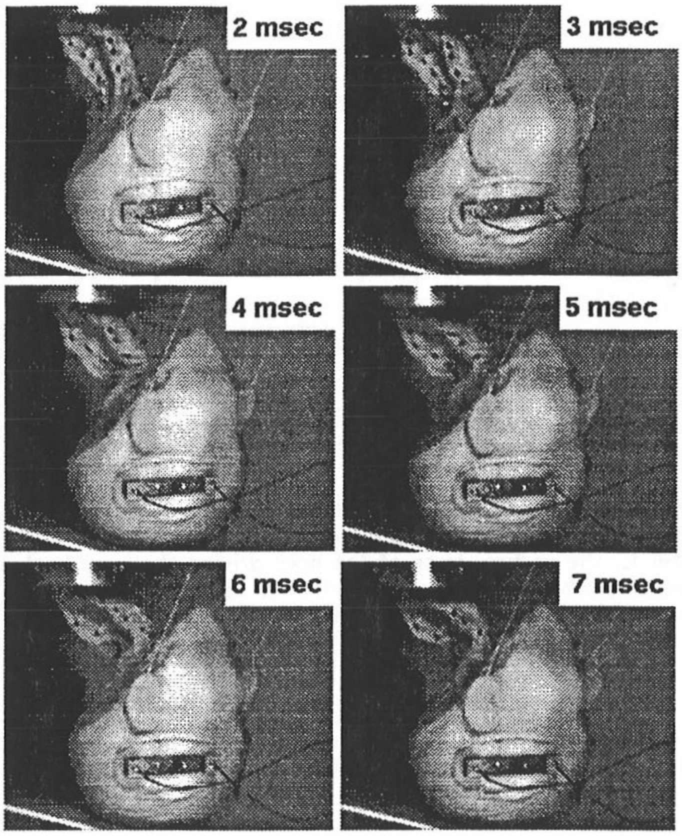

FIGURE 5 High speed digital images of a rigid impact at -15° illustrating buckling effects (the images have been modified to exclude facial features). The images show the normal lordotic curve (2 msec), followed by a transient higher order mode (3 msec) which decays quickly (4 msec) to a first order buckle (5 msec). The buckle is then stable (non-injurious) and results in a characteristic post buckled deformation including regions of flexion, extension, and compression within the cervical spine.

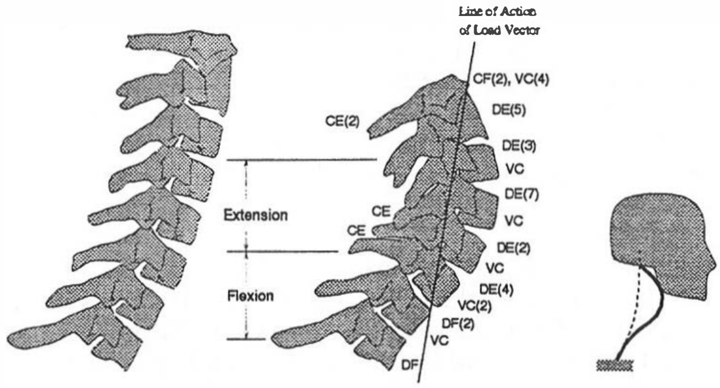

FIGURE 6 Schematic illustration of the postbuckled spine, showing a representative location of the resultant force and the injury distribution. Unlike head motion, the post-buckled deformation and resultant force location are able to explain the mechanism and patterns of injury. (CF = compressive flexion, CE = compressive extension, VC = vertical compression, DE = distractive extension, DF = distractive flexion)

Each of the basilar skull fractures occurred during the neck-loading mode (Mode 2) of the impact (Figure 3). Specifically, using the defined injury criteria and combining the kinematic and kinetic data sets, basilar skull fractures occurred 15.4±3.2 msec following peak impactor force. Head Injury Criteria for the rigid and two padded basilar skull fractures were 1935, 90, and 119, respectively. Time corridors (T1 and T2) selected to maximize the HIC calculation fell within the head inertial loading mode (Mode 1) for each of the three injuries. Thus, the time range used in the HIC calculation did not include the time at which the skull fractures occurred. The axial (spatially fixed, superior-inferior direction) neck forces to produce the fractures were -2494, -2126, and -2085 N for the rigid and padded injuries (mean = -2235±225 N). The axial forces required to produce basilar skull fracture were larger than the forces required to produce the concurrent cervical injuries in each of the three cases (Table 2).

Padding was found to significantly increase the risk for injury and to increase the severity of injury. Using the groups of data in which both rigid and padded impacts were performed, we found that all nine of the padded impacts and four of the nine rigid impacts produced cervical spine injury (Table 3). Performing an ANOVA on these data, we found that the frequency of injury in the padded impacts was significantly greater than the frequency of injury in the rigid impacts ($p=0.0375$). In the same context, only two of the rigid impacts were found to be clinically unstable, while seven of the nine padded impacts were unstable.

TABLE 3: Injury Frequency and Severity

	Rigid Impacts		Padded Impacts	
	Injured	Unstable	Injured	Unstable
Anterior	2/3	1/3	3/3	3/3
Vertex	2/3	1/3	3/3	3/3
Posterior	0/3	0/3	3/3	1/3
Total	4/9	2/9	9/9	7/9

For the rigid impacts, the axial impulses were 41.0±14.2 N-s. For the padded impacts, the axial impulses were 60.2±21.9 N-s. The axial impulses were grouped based on impact angle and impact surface in order to perform a two-way analysis of variance. The impulses in the padded impacts were significantly larger than the impulses in the rigid impacts ($p=0.00023$). Two-way ANOVA also found significant differences between axial impulses as a function of impact angle ($p<0.0001$) with the posterior impacts produced the smallest impulses and the anterior and vertex impacts produced larger impulses (Table 1).

Padding significantly lowered the risk for head injury. Peak resultant head force applied by the impact surface was significantly lower for the padded impacts, -4127±1375 N, than for the rigid impacts, -8297±1572 N ($p=0.02$). Similarly, the average HIC for the padded impacts, 136±32, was significantly lower than the average HIC for the rigid surface, 1010±534. Average axial neck force to produce the first neck injury was -1948±666 N and did not vary with impact surface.

DISCUSSION

Catastrophic head impact neck injury remains a significant societal problem. As a direct result, a large volume of literature has been written on neck injury in which static relationships between head motion and neck injury are hypothesized. Unfortunately, as in the case presented herein, real world cases often present with findings which cannot be explained using this static approach. This suggests that neck injury is the result of the dynamic responses of a more complex mechanical system. With this in mind, the purpose of this investigation is to understand the dynamics of head impact neck injury, to create a mechanical paradigm in which the responses of the neck are better understood, and to allow a rational investigation of strategies for neck injury prevention.

Central to the testing of any hypothesis is the demonstration of the impact model's validity. Using our experimental apparatus, we produced a variety of clinically observed injuries, including Jefferson fractures, Hangman's fractures, burst fractures, posterior element fractures, bilateral facet dislocations, and basilar skull fractures. The injuries in this study were produced in the absence of preflexion (i.e. the normal lordosis of the spine was preserved). Additionally, the distribution of injuries produced is consistent with the distribution of injuries reported in epidemiology studies (Myers and Winkelstein, 1995).

These data illustrate the ease with which the neck may be injured, and illustrate how neck injuries can occur with the pelvis properly and fully restrained owing only to the mass of the uppermost portions of the torso. Six of the specimens suffered no injuries while 16 were injured using an impact velocity of 3.1 m/s. This was consistent with the measurements by McElhaney et al. (1979) in which a head impact velocity of 3.1 m/s was thought to be a critical velocity for neck injury. Importantly, our model used an effective dynamic torso mass of only 16 kg, which represents only approximately 40% of the isolated torso mass of a 50th percentile male.

In considering only head and neck injury potential, the impact may be regarded as a one body problem involving the deformation of a neck spring beneath an effective dynamic torso mass. The lag between the neck load and the head load indicates that the torso and neck are poorly coupled. Therefore, the spring should be nonlinear, show an initial low stiffness region, and stiffen with increasing deformation (Myers et al., 1991). With this model, injury potential exists when the head is constrained and the neck is called upon to stop the moving torso. Interestingly however, two of the impacts to rigid, low friction surfaces resulted in catastrophic spinal injuries. Thus, injury was produced in the complete absence of constraints imposed by the contact surface. This differs from static studies which were unable to produce compression neck injuries in the absence of a constrained head end condition (Myers et al., 1991, Roaf, 1960), and is explained by the inertial loads imposed by the head. Specifically, these experiments show that in addition to managing the momentum of the torso, the neck must also accelerate the head out of the path of the torso. They also show that head rebound from the impact surface creates a significant portion of the neck load. In that regard, neck injury must be modeled as a two body problem in which neck loads are generated by the torso mass, the impact surface and the head mass.

As in prior studies, head motion was unrelated to injury mechanism (Nusholtz et al., 1983). This occurred in part because the head motion lags the applied forces which produce injury, and does not occur until well after neck injury. Also not explained by head motion, is the frequent occurrence of multiple noncontiguous injuries of differing mechanisms at different levels within the spine. This was seen in the case study (Figure 1), and also seen in the experimental data, including specimen N18, whose injury distribution and point of impact are identical to those presented in the case study. Returning to the mechanical model of the segmented beam column helps to explain these otherwise paradoxical observations. These experiments show that the spine acts as a slender, curved beam column with a fixed base and pinned apex. Once a critical load is reached, this structure snap-through buckles with a rapid transition from a predominantly compression mode of deformation to a predominantly bending mode of deformation (Figure 6). As in prior static studies (Myers et al., 1991), the cervical spine shows post-buckling stability, as it can be buckled without injury. Thus, buckling is a structural failure and not a material failure (a neck injury). While buckling is not injury, the post-buckled mode shape does explain the mechanism of these injuries. The buckled deformation exhibits regions of extension in the middle cervical spine and flexion in the lower cervical spine. As a result, the neck load vector passes behind the middle cervical spine and causes compression-extension, and in front of the lower cervical spine and causes lower cervical compression-flexion. Thus, by treating the spine as a seven segment beam column which is sufficiently slender to buckle, interposed between the torso and head masses, the relationships between the point of head impact and the type of neck injuries produced becomes well defined.

While able to explain the injuries seen in this study, the first order buckle does not explain the production of midcervical (C3 to C6) flexion injuries. Yet clinical studies show that this is a common injury. Additionally, previous research has demonstrated that preflexion may be one mechanism for producing midcervical compression-flexion injuries (McElhaney et al., 1983, Pintar et al., 1990, Torg et al., 1990). Another, mechanism of midcervical flexion injuries may be the development of higher order buckling modes (Figure 5). In these experiments, the higher order mode shape, which produces midcervical flexion decayed prior to injury. Using a numerical model validated against these experiments (Nightingale et al., (submitted); Camacho et al., (submitted)), showed that the buckled mode shape is most dependent on the flexion-extension flexibility of the spine, and that this higher order mode is expressed because of the inertial forces developed in each of the vertebral masses during the snap-though motion (Figure 7). It is possible that at higher impact velocities, in which the torso loads the neck more rapidly, injury may occur during this higher order mode, and result in midcervical compression flexion injuries.

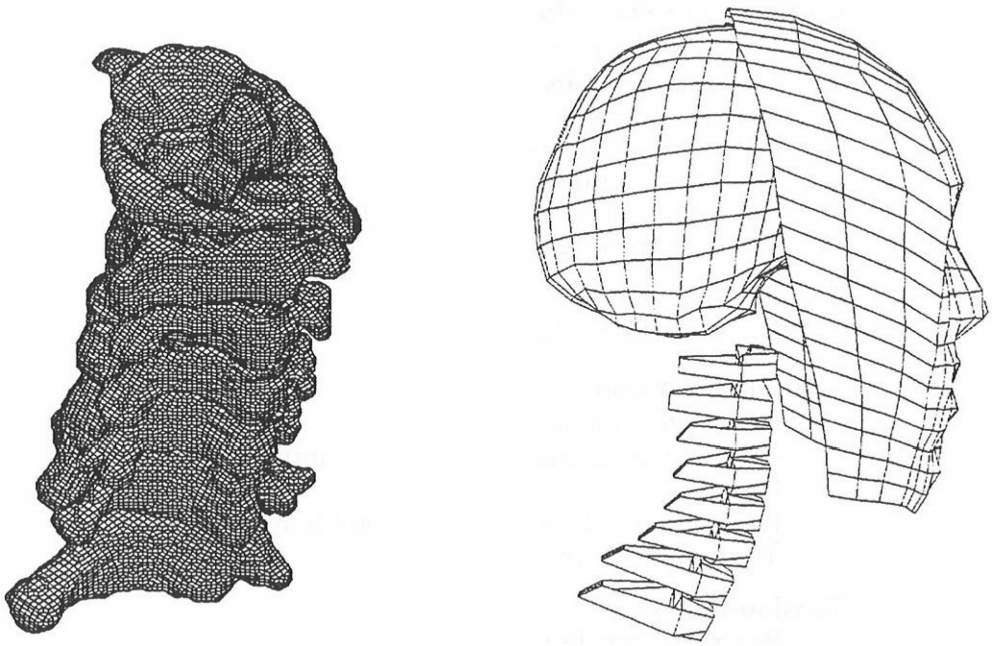

FIGURE 7 Posterolateral (left) views of the cervical vertebrae reconstructed from axial CT images (Camacho et al., 1998). From these meshes, the centroid position, mass, and sagittal plane moment of inertia were calculated for each vertebra. The Hybrid finite element head/multibody dynamics neck model (right) was derived from the reconstructed mesh and spinal flexibility data (Nightingale et al. submitted). A rigid face was coupled to the rigid maxilofacial region of the skull and assigned mass properties such that the mass, moment of inertia, and centroid of the entire head matched the data of Walker et al. (1973). Validated against the drop test data, this model shows that the expression of the higher order buckling mode is the result of inertial forces from the small masses of each vertebrae which oppose the expression of the first mode buckle.

It well recognized that the spine is a complex geometric structure with nonlinear, rate dependent responses. The results of our studies suggest the need for a more complex mechanical paradigm. That is, by considering the effective dynamic torso mass, the head mass, the nonlinear curved slender segmented beam column and each of the vertebral masses, the dynamic responses of the spine can be more fully understood. Additionally, by organizing the neck injury literature according to this paradigm, a coherent understanding of neck injury mechanisms and injury classification emerges. Specifically, at the time of injury, a resultant force with some eccentricity acts on the spine at the

TABLE 4: Cervical Spine Injuries: A Classification Based on Applied Forces with Experimental Validation

Compression
- Jefferson fracture
- Multipart atlas fracture
- Vertebral body compression fracture
- Teardrop fracture

Compression-flexion
- Teardrop fracture
- Burst fracture
- Wedge compression fracture
- Hyperflexion sprain
- Bilateral facet dislocation
- Unilateral facet dislocation

Compression-extension
- Hangman's fracture
- Clay-shoveler's fracture
- Posterior element fracture
- Anterior longitudinal ligamentous rupture
- Anterior disc rupture
- Horizontal vertebral body fracture
- Teardrop fracture

Tension
- Occipitoatlantal dislocation

Tension-extension
- Hangman's fracture
- Anterior longitudinal ligamentous rupture
- Disc rupture
- Horizontal fracture of the vertebral body
- Teardrop fracture

Tension-flexion
- Bilateral facet dislocation
- Unilateral facet dislocation

Torsion
- Atlantoaxial rotary dislocation
- Unilateral atlantoaxial facet dislocation

Shear
- Odontoid fracture
- Transverse ligament rupture

Lateral Bending (in combined loading)
- Asymmetric injury
- Nerve root avulsion
- Peripheral nerve injury

point of injury. By considering this load as a force and an associated couple, a clear relationship between neck resultant force and injury is produced (Table 4).

Interestingly, three ring type basilar skull fractures were observed among 16 specimens with injuries, an incidence of 18.7%. This suggests that basilar skull fractures are a common consequence of near vertex head impact. In each case, the skull fractures were accompanied by cervical injuries and the skull fractures occurred at forces slightly larger than those required to produce the cervical injuries in the same specimens. Yoganandan et al. (1986) reported four skull fractures from head impacts. Three of these had concurrent cervical injuries, including the one specimen with a true basilar skull fracture (i.e. without cranial vault injuries). Alem et al. (1984) reported a case of a basilar skull fracture as a result of head impact, and did not detect other cervical injuries. These results suggest that the skull base may have a slightly larger force tolerance than the cervical spine. As a result, compression mediated basilar skull fracture will more often than not be associated with cervical injury.

Alem et al. (1984) was among the first to report basilar skull fracture as a result of near vertex head impact. Based on their observations, it remained unclear if basilar skull fractures were the result of head impact acceleration or neck loading. By measuring neck and impact surface forces, our study demonstrates that basilar skull fractures occur toward the end of the dynamic event in the neck impact surface loading mode. At this time, the head is compressed between the cervical spine and the impact surface, and head inertia is small. In that regard, basilar skull fracture as a result of near vertex head impact represents a quasi-static failure mechanism which is unrelated to the head acceleration. It is also, therefore, unrelated to head acceleration based injury criterion like the HIC. In this context, basilar skull fractures may be thought of mechanistically as a fracture of the C1 motion segment of the cervical spine. This has implications for injury prevention. Specifically, while head injuries are readily mitigated by the addition of surface padding (as measured by a decrease in HIC), neck injuries are insensitive to, and perhaps potentiated by the addition of surface padding. Thus, it is unlikely that addition of padding to an impact surface will prevent basilar skull fracture as a result of near vertex head impact. Additionally, basilar skull fracture can occur at drop heights of 0.53 m, a height at which skull fractures are uncommon, however, cervical injuries are common. It should be recognized that these fractures occur through other mechanisms however, and that these other mechanisms may be governed by other tolerance criterion.

The effects of padding on injury risk were examined in this study by simulating extremes in impact surface properties from rigid, low friction, unconstrained surface to a highly deformable, pocketing surface. The materials used in this experiment are more compliant than those paddings and liners that are currently in use by the automotive and other safety industries. Analysis of the injury data shows that there was a significantly greater frequency of injury in the padded impacts than in the rigid impacts ($p=0.0375$). This shows that pads do not protect the neck and supports the hypothesis that padded surfaces may increase the risk of cervical spine injury. The effect of padding on injury risk was particularly apparent in the posterior impacts: none of the rigid impacts produced injury, and all of the padded impacts produced injury. In the padded posterior impacts, the head and neck have an initial component of velocity in the anterior direction relative to the impact surface. The anterior components of forces applied to the head by the impact surface and by the neck, increase the escape velocity. These were sufficient to move the head out of the path of the following torso before injurious loads could develop in the neck. However, in the experiments where a padded surface was used, the deformed pad applied posteriorly directed forces which decreased the anterior head escape velocity. As a result, the neck was subjected to significantly more of the torso momentum ($p=0.00023$); that is, the neck was forced to stop the moving torso, and the neck sustained more injuries which tended to be more severe. Importantly, the surface padding used in this study was able to significantly reduce the magnitude of the measured head impact force and therefore the risk for head injury. HIC values were reduced from an average of 1045 to an average of 159. Thus, this padding surface protected the head and did not protect the neck. Therefore, these experiments suggest that highly deformable padded contact surfaces should be employed carefully in environments where there is the risk for cervical spine injury. In addition, the results suggest that the orientation of the head, neck, and torso relative to the impact surface is of equal if not greater importance in neck injury risk. Additional research and a large number of specimens is necessary to identify which head and neck positions and impact angles are most likely to produce injury, and which padding materials and material thickness provide the optimal balance between head protection and neck protection. Given the prohibitive cost of cadaver studies, perhaps these questions will be best answered using a computational model.

The results of our impact studies, together with the works of others comprise almost 50 human head and neck studies in which adequate instrumentation are available to characterize the neck loads at the time of injury (Yoganandan et al., 1986, Pintar et al., 1995). In that regard, they serve as a database for the formulation of a human cervical tolerance. Among the important variables for defining this tolerance are gender and the presence of preflexion. That is, the male cervical spine is stronger than the female spine (Nightingale et al., 1997b), and preflexion, which minimizes bending stresses, requires larger forces to failure than a neutrally positioned spine. Also important, thought not well characterized, is the significance of age related changes and the possible gender differences of these changes. Not surprisingly, the methods by which these variables are accounted for can influence the estimated tolerance. Combining data sets with preflexed and neutral spines as well as men and women donors, we have suggested a resultant force tolerance to near vertex head impact of 2.75 to 3.44 kN (Myers and Winkelstein, 1995). More recent analyses of these data using only males, both preflexed and neutral, suggested a tolerance of the young adult male between 3.58 to 3.73 kN (Nightingale et al., 1997b).

CONCLUSIONS

1. Neck injuries are commonly produced at velocities of 3.1 m/s with an effective dynamic mass of only 40% of the total torso mass.

2. Head and neck dynamics include a bimodal response of a head impact mode, and a neck impact surface loading mode. Characteristic features of this response include the poor coupling of the head and neck owing to an initial low neck stiffness, and head rebound.

3. Head motion is unrelated to the neck injury mechanism as neck injuries occur prior to significant head motions.

4. The cervical spine buckles as a result of head impact. The buckle is not an injury, however, the post-buckled mode shape is able to explain the distribution of neck injuries, and the relationship between head forces and neck injuries.

5. Higher order buckling modes can be observed in the spine and are the result of inertial loads in each of the vertebral bodies.

6. Basilar skull fractures are a common, difficult to detect, consequence of compression neck loading. The injury behaves mechanistically like a neck injury as it occurs during the neck impact surface loading mode, and it is described by a neck load measurement and not a head acceleration criterion.

7. Cervical spine injuries can be classified by examining the location of the resultant force on the motion segment.

8. Constraint of head motion due to pocketing in a highly deformable padded surface may increase the risk of cervical spine injury; however, the orientations of the head, neck, and torso relative to the impact surface are of equal if not greater importance. These pads significantly reduce peak head forces and therefore reduce head injury risk. Determination of an optimum pad is the subject of ongoing investigations.

9. Sufficient data are available for the formulation of a meaningful near vertex head impact tolerance for the neck; however, the tolerance is a function of a number of different variables, and several methods exist to combine these data into an average human tolerance. One such analysis suggests a resultant tolerance of 3.58 to 3.73 kN for the young adult male.

10. Head impact neck injury should be modeled as the dynamic response of two large masses coupled by a segmented curved beam-column comprised of seven small masses with interposed nonlinear viscoelastic flexibility elements. Though complex, this approach creates a cogent relationship between head impact, head motion, buckling dynamics, injury classification, injury mechanism, and injury prevention and is able to explain the often confounding clinical presentation of cervical spinal injuries.

ACKNOWLEDGMENTS

Research in the Injury and Orthopaedic Biomechanics Laboratory has been provided by the the Department of Transportation NHTSA Grant, DTNH22-94-Y-07133, the Department of Health and Human Services CDC Grant, R49/CCR402396-10, the National Science Foundation, and the National Institutes of Health, MSTP program. The views and opinions expressed in this paper are those of the author and do not necessarily represent those of the funding organizations. A large number of dedicated and capable investigators have made contributions to the research presented herein. The most longstanding and significant is that of Dr. James McElhaney. Significant contributions have been made by Drs. William Richardson, Linda Gray, Tom Best, Brian Doherty, Robert Hopper, and Jacqueline Paver. Significant contributions have also been made by Chris Van Ee, Danny Camacho, Beth Winkelstein, Todd Woolley, Judge Robinette, and James Yu.

REFERENCES

Alem, N.M., Nusholtz, G.S., Melvin, J.W., "Head and neck response to axial impacts". *Proceedings of the 28th Stapp Car Crash Conference*, SAE Paper 841667, 927-940 1984.

Camacho, D.L.A., Nightingale, R.W., Robinette, J.J., Vanguri, S.K., Coates, D.J., Myers, B.S., "Flexibility measurements for and validation of a computational head-neck model for near-vertex head impact". *Proceedings of the 41th Stapp Car Crash Conference*, (submitted).

Camacho, D.L.A., Hopper, R.H., Myers, B.S., "An improved method for finite element mesh generation of geometrically complex structures with application to the skullbase". *Journal of Biomechanics*, in press, 1998.

Cavanaugh, J.M., King, A.I., "Control of transmission of HIV and other bloodborne pathogens in biomechanical cadaveric testing". *Journal of Orthopaedic Research*, 8:159-166, 1990.

Harris, J.H., Eideken-Monroe, B., and Kopaniky, D.R., "A practical classification of acute cervical spine injuries". *Orthopaedic Clinics of North America*, 17:15-30, 1986.

Hodgson, V.R., Thomas, L.M., "Mechanisms of cervical spine injury during impact to the protected head". *Proceedings of the 24th Stapp Car Crash Conference*, SAE Paper #801300, 17-42, 1980.

Matsuchita, T., Sato, T.B., Hirabayashi, K., Fujimura, S., Asazuma, T., Takatori, T., "X-Ray study of the human neck motion due to head inertia loading". *Proceedings of the 38th Stapp Car Crash Conference*, SAE Paper #942208, 55-64, 1994.

McElhaney, J.H., Paver, J.G., McCrackin, H.J., Maxwell, G.M., "Cervical spine compression responses". *Proceedings of the 27th Stapp Car Crash Conference*, SAE Paper #831615, 163-177, 1983.

McElhaney, J., Snyder, R.G., States, J.D., and Gabrielsen, M.A., "Biomechanical analysis of swimming pool neck injuries". *Proceedings of the 23rd Stapp Car Crash Conference*, SAE Paper #790137, 494-500, 1979.

Mertz, H.J., Hodgson, V.R., Thomas, L.M., and Nyquist, G.W., "An assessment of compressive neck loads under injury-producing conditions". *Physician and Sportsmedicine*, 6(11):95-106, 1978.

Myers, B.S., Richardson, W.J., Doherty, B.J., Nightingale, R.W., McElhaney, J.H., "The role of head constraint in the development of lower cervical compression flexion injury". *Proceedings of the 35th Stapp Car Crash Conference*, SAE Paper #912915, 391-399, 1991.

Myers, B.S., Winkelstein, B.A., "Epidemiology, classification, mechanism and tolerance of human cervical spine injuries". *Critical Reviews in Biomedical Engineering* 23(5&6):307-409, 1995.

Myers, B.S., Nightingale, R.W., "Basilar skull fracture reslting from compressive neck loading". *AGARD Specialist Meeting on Impact Head Injury*, Mescalero, New Mexico, in press, November, 1996.

Nightingale, R.W., McElhaney, J.H., Richardson, W.J., Best, T.M., Myers, B.S., "Experimental impact injury to the cervical spine: relating motion of the head and the mechanism of injury". *Journal of Bone Joint Surgery*, 78-A(3): 312-321, 1996a.

Nightingale, R.W., McElhaney, J.H., Richardson, W.J., Myers, B.S., "Dynamic responses of the head and cervical spine to axial impact loading". *Journal of Biomechanics*, 29(3): 307-318, 1996b.

Nightingale, R.W., Richardson, W.J., Myers, B.S., "The effects of padded surfaces on the risk for cervical spine injury". *Spine*, (accepted), 1997a.

Nightingale, R.W., McElhaney, J.H., Camacho, D.L., Winkelstein, B.A., Myers, B.S., "The dynamic responses of the cervical spine: the role of buckling, end conditions, and tolerance in compressive impacts". *Proceedings of the 41th Stapp Car Crash Conference*, 1997b.

Nightingale, R.W., Camacho, D.L., Armstrong, A., Robinette, J.J., Myers, B.S., "Cervical spine flexibility and the effects of vertebral mass and loading rate on cervical spine buckling dynamics". *Journal of Biomechanics*, (submitted).

Nusholtz, G.S., Huelke, D.E., Lux, P., Alem, N.M., Montalvo, F., "Cervical spine injury mechanisms". *Proceedings of the 27th Stapp Car Crash Conference*, SAE Paper #831616, 1983.

Panjabi, M.M., White, A.A. 3d, Johnson, R.M., "Cervical spine mechanics as a function of transection of components". *Journal of Biomechanics*, 8(5):327-36, 1975.

Pintar, F.A., Sances, A. Jr., Yoganandan, N., Reinartz, J., Maiman, D.J., Suh, J.K., Unger, G., Cusick, J.F. and Larson, S.J., 'Biodynamics of the total human cadaveric cervical spine". *Proceedings of the 34th Stapp Car Crash Conference*, SAE Paper #902309, 1990.

Pintar, F.A., Yoganandan, N., Pesigan, M., Voo, L., Cusick, J.F., Maiman, D.J., Sances, A. Jr., "Dynamic characteristics of the human cervical spine". *Proceedings of the 39th Stapp Car Crash Conference*, SAE Paper #95722, 195-202, 1995.

Roaf, R., "A study of the biomechanics of spinal injuries". *Journal of Bone Joint Surgery*, 42B(4): 810-23, 1960.

Torg J.S., Quendenfeld, T.C., Thieler, E.R. III, et al., "Collision with spring-loaded football tackling and blocking dummies". *Journal of the American Medical Association*, 236:1270-1271, 1976.

Torg J.S., Vegso, J.J., O'Neill, M.J., Sennett, B., "The epidemiologic, pathologic, biomechanical, and cinematographic analysis of football-induced cervical spine trauma". *American Journal of Sports Medicine*, 18(1):50-57, 1990.

Walker, L.B.Jr., Harris, E.H., Pontius, U.R., "Mass, volume, center of mass, and mass moment of inertia of head and neck of the human body". *Proceedings of the 17th Stapp Car Crash Conference*, 525-37, 1973.

Yoganandan, N., Sances, A. Jr., Maiman, D.J., Myklebust, J.B., Pech, P., and Larson, S.J., "Experimental spinal injuries with vertical impact". *Spine*, 11(9):855-860, 1986.